Analysis and investigations on a digitally controlled LED buck driver for automotive LED applications

Emil N. Kovatchev, Nadezhda L. Evstatieva

This article presents a configurable constant current LED driver with DSP digital control. A novel, cost-effective high-side current sensing circuit provides feedback signal, proportional to the average LED current. A fast PID controller is implemented on a microcontroller with DSP core. The PID controller drives a fully integrated half-bridge IC in a synchronous step-down configuration. A prototype PCB has been designed and thoroughly investigated. The PID parameters have been adjusted according to the Takahashi PID tuning method. The performance of the tuned LED controller has been evaluated in terms of stability, steady-state precision, transient response and efficiency.

Анализ и изследване на светодиоден (LED) драйвер с понижаващ преобразувател на напрежение за автомобилни приложения (Емил Н. Ковачев, Надежда Л. Евстатиева). *Тази статия представя светодиоден (LED) драйвер с DSP-микроконтролерно управление. Иновационна, икономически ефективна схема на токов монитор предоставя сигнал, пропорционален на светодиодния ток. Бърз пропорционално-интегрално-диференциален (ПИД) - регулатор е реализиран цифрово чрез микроконтролер с DSP-копроцесор. ПИД - регулаторът управлява два MOSFET транзистора, конфигурирани като синхронен понижаващ преобразувател (syncronous buck converter). Прототип на предложения светодиоден драйвер е реализиран и обстойно изследван. ПИД - параметрите са оптимирани по метода на Takahashi. Настроеният ПИД – регулатор е изследван по отношение на стабилност, точност в стационарен работен режим, импулсен отговор и ефективност.*

Introduction

The automotive power LED light applications – e.g. high and low beam, fog lights, positioning light, tail lights, brake lights - are gaining momentum due to their undisputed advantages – long life expectation, high efficiency, compact solid state construction and elegant design.

A properly designed LED driver acts as a constant current source which raises its output voltage until the desired LED current target is met and maintains regulation, compensating for possible LED forward voltage fluctuations by engaging a fast current regulation loop.

The closed loop control is commonly based on the proportional-integral-derivative (PID) control law. In purely analog LED controllers, the P, I and D terms are adjusted by resistors and capacitors, placed properly in the feedback of the error amplifier in order to define poles and zeroes and shape the closed loop transfer function in the desired manner. Examples include the integrated LED drivers TL5098 by Infineon [1], LT3755 by Linear Technology [2], MAX16833 by Maxim [3]. These ICs feature a transconductance amplifier in the feedback loop. The output of this amplifier acts as a current source, the RC compensation network can thus be placed between output and ground.

The analog solutions do not allow for flexible feedback loop shaping due to the need for component value modifications. The discrete component values do not allow for exact definition of the PID-coefficient, thus an iterative approach is required. The aging and the tolerances of the power plant components cannot be compensated for.

With the advance of the digital signal processing, discrete PID control algorithms have been implemented on a fast digital core [4]. The advantages of the digital solutions include the easy loop response tuning, the adaptive control algorithms depending on actual operation point (e.g. using individual PID coefficient sets for start-up with minimum overshoot, steady state with precise set-point regulation, fast load step and transient response, shut-down with no oscillations), the auto tuning ability, which enables automatic compensation for aging components.

Goals and tasks

The objective of the present paper is the design, analysis and experimental verification of a precise, highly integrated, digitally controlled LED driver for automotive applications. Special attention is given to the PID coefficient tuning procedure, the transient- and stability analysis.

The advantages of the proposed solution include:

- a novel, cost-effective and precise high - side current measurement circuit, thoroughly described in [5], used for LED average current sensing and closing the feedback loop;
- a simple and fast discrete PID algorithm with integral anti-windup, which enables the use of low-cost microcontrollers;
- the use of highly integrated power driver stage DRV8412 which allows for high switching frequency, low switching losses, simple single-ended PWM control for a half-bridge, on-chip LED overcurrent protection and diagnostics;

Design goals are output power of 30W, LED current 0.2A…1A, supply voltage <50V, steady state error of <5%, phase margin >45%, transient response <50µs, overshoot <10%, efficiency >86%.

Presentation

A synchronous step-down converter topology has been selected for the LED controller, due to the following considerations:

- regulated 42…45V link voltage (which is also the input voltage for the LED driver presented here) is already available in the conceptual LED control module by employing a multi-phase boost converter;
- the high LED current needed in front lighting application, but also the lightweight construction of modern cars, demand for high efficiency and low weight, which implies a low-loss synchronous rectification for the power converters.

PID controller basics

The proportional-integral-differential (PID) controller has been well established and investigated for decades and is widely used in the electrical engineering. It combines a robust control theory fundament with the somehow intuitive tuning approach [6]. The sum of three corrective terms - proportional, integral and differential - determines the output of the controller:

P-term – the proportional response determines the magnitude of the output response as a function of the error. Higher proportional gains increase the speed of the control system, but also produce overshoots and – eventually - control loop oscillations which may even destroy the control system;

I-term – the integral term sums up the errors over time. It stores the error information from the past - the magnitude of the integral increases even with small deviations from the set point. The PID controller needs this information in order to drive the steady state error to zero. Setting the integral term too high slows down the response of the control loop;

D-term – the differential term is proportional to the rate of change of the output. It will force the system to react faster to changes in the error signal and increase the response speed of the system. Care must be taken when using the derivative term since it is highly sensitive to noise.

Depending on the control system demands, partial variations of the full-featured PID controller are also possible, e.g.: PD controllers are used for power plants with integrator behavior (motors, heating elements); PI controllers are used for cost efficient regulation where no tight control or fast transient response is required.

The LED automotive driver presented in this work has to comply with rigorous transient test pulses specified in standardized automotive regulations (superimposed sinus sweeps, inductive transient spikes, load-dump, jump start pulses) and also maintain tight LED current regulation of typically +/-5% over automotive temperature and battery supply range. Therefore a full-featured, fast and precise PID controller has to be designed.

PID controller design

As a starting point, the actual error, i.e. the difference between the desired set-point and the actual value of the control variable, has to be determined. For the LED driver presented in Figure 1, the error signal is the difference between the targeted LED current I_{set} and the actual LED current I_{out}. Since the PID controller samples the output voltage of the high-side current monitor $V_{sense}(t)$, which is directly proportional to the LED current, as stated in [5], a virtual reference V_{set}, proportional to the setpoint current I_{set} is fed into the PID controller:

(1) $$V_{set} \propto I_{set}, V_{sense} \propto I_{out},$$

The error signal then becomes:

(2) $$e(t) = V_{set} - V_{sense}(t),$$

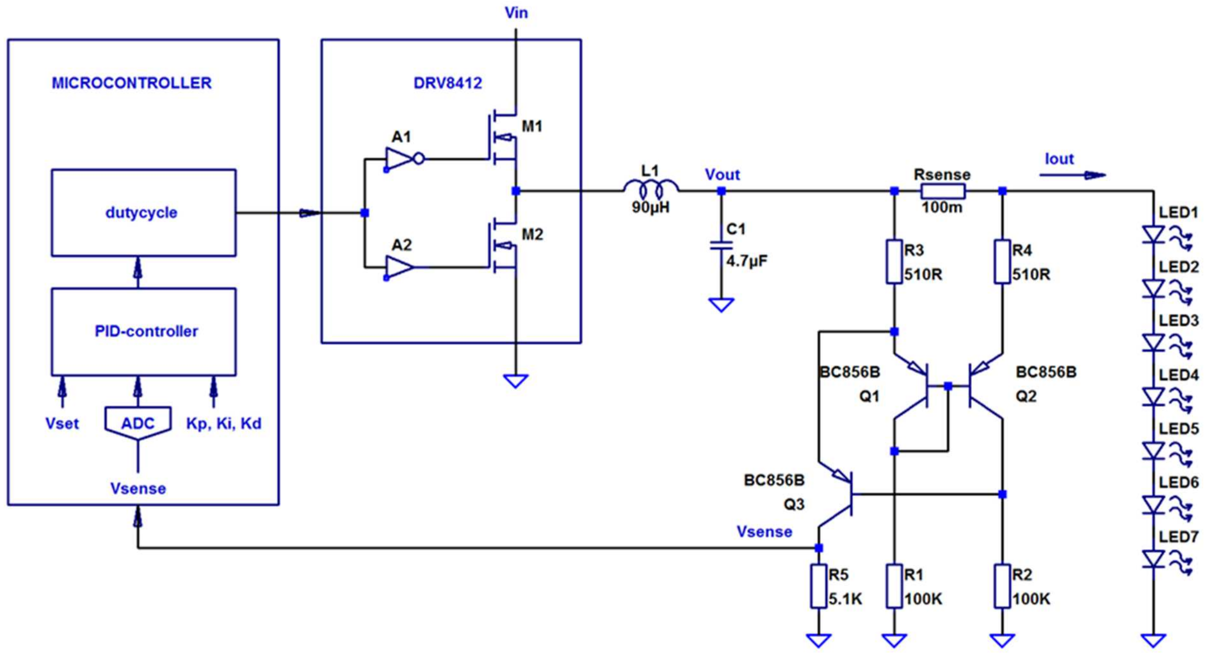

Fig. 1. Schematic of the proposed digital PID-controller for LED applications.

Considering the fact, that the output variable of our LED controller is represented by the duty cycle of the buck FET, the PID control law in the time domain can be expressed by the following equation:

$$duty(t)=K_p e(t)+K_I\int_0^t e(\tau)d\tau+K_D\frac{de(\tau)}{dt}, \tag{3}$$

In alternative notation, related to the time constants of the integral and differential blocks:

$$duty(t)=K_p\left\{e(t)+\frac{1}{T_I}\int_0^t e(\tau)d\tau+T_D\frac{de(\tau)}{dt}\right\}, \tag{4}$$

where K_p is proportional gain, K_I is the integral gain, K_D is the derivative gain, T_I is the integral time constant, T_D is the derivative time constant, τ is an integration variable.

For a digital PID controller implementation the equation (4) has to be transformed in the discrete time domain using the forward (rectangular) Euler integration method [7]:

$$duty(n)=K_p\left\{e(n)+\frac{T_S}{T_I}\sum_{i=0}^{n-1}e(i)+\frac{T_D}{T_S}\left(e(n)-e(n-1)\right)\right\}, \tag{5}$$

where n is the discrete time sampling instant, T_S is the sampling time.

In equation (5), the products $K_p\frac{T_S}{T_I}$, $K_p\frac{T_D}{T_S}$, as well as K_p are constants (provided the sampling intervals are also constant) and shall be tuned properly for fast response and stability.

Care must be taken to limit the output variable (the duty cycle of the power FETs) to safe value and also prevent a potential runaway of the integral error sum by implementing an “anti-windup” limit check.

A detailed signal flow diagram of the proposed digital PID controller, including integral anti-windup, is depicted on Figure 2, whereas *v_set* denotes the LED current setpoint, *v_sense[n]* is the discretized LED current monitor signal, *e[n]* is the discrete error signal, *ε* is the dead-band region, *d[n]* stands for the updated duty cycle after the PID-controller execution.

PID controller tuning

The purely analytical P, I, D coefficient calculation of the digital controller requires a thorough knowledge of the power plant and regulation loop characteristics, which is often unavailable.

Therefore, PID control tuning procedures based on experiments and simplified calculations have been developed, e.g. by Ziegler-Nichols (ZN) [8], Takahashi [9] and others [10]. These methods rely partially on experiments with the closed loop system, in which the control output is brought to oscillations by setting the integral and derivative term to zero and increasing slowly the proportional gain only until instability

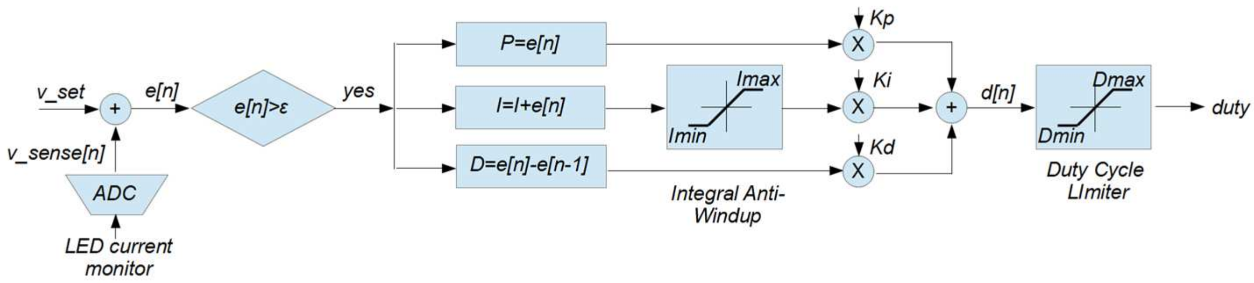

Fig.2. Block diagram of the digital PID controller with anti-windup algorithm.

occur. Obviously, these methods are only applicable for control systems where the oscillations do not overstress or damage the control loop- and power plant components.

The Ziegler-Nichols tuning method results in a rather aggressive gain and overshoot prediction and also requires knowledge of the oscillation frequency, whereas the Takahashi method only requires the knowledge of the minimum gain, K_{OSC}, at which the oscillation starts.

For the purposes of this paper we will use the Takahashi PID tuning method due to the moderate stress it poses on the control system.

For discrete PID controller, [11] states that the sampling time T_S of the control process shall comply with the condition

(6) $$T_S \approx \frac{T_{settling}}{5 \div 15},$$

where $T_{settling}$ represents the settling time of the output within 95% of its nominal value. $T_{settling}$ has been measured to be approximately 50μsec, the switching frequency of the buck converter is set in the range 210kHz … 250kHz.

A sampling time of 4μsec allows the FET duty cycle to be updated in the next switching cycle. Setting T_S to 4μsec fulfils condition (6) well. A longer sampling time will degrade the phase margin (thus the stability) of the system.

According to [9], for known K_{OSC} and T_S the PID-coefficients can be calculated in following manner (Table 1).

To determine the critical K_P gain, the buck output is brought to oscillations by observing the converter output voltage with an oscilloscope, setting the integral and derivative term to zero and slowly increasing the proportional gain until output voltage instability occurs. The experimentally determined minimum gain K_{OSC} at which the oscillations on output of the PID controller occur, is

(7) $$K_{OSC} = 1.041.$$

The initial coefficients for the digital PID controller have been calculated according to the equations in Table 1, considering the sampling time $T_S = 4\mu s$ and the measured value for K_{OSC}:

(8) $$K_P \approx 0.499, \frac{T_S}{T_I} = 0.250, \frac{T_D}{T_S} = 0.015$$

Table 1

Experimental tuning with stability limit experiments. Takahashi [9]

Controller Type	K_P	$\frac{T_S}{T_I}$	$\frac{T_D}{T_S}$
P	$0.5K_{osc}$	*n.a.*	*n.a.*
PI	$K_{osc}\left(0.45 - 0.27\frac{T_S}{T_{osc}}\right)$	$K_{osc}\left(0.45 - 0.27\frac{T_S}{T_{osc}}\right)$	*n.a.*
PID	$0.6K_{osc}\left(1 - \frac{T_S}{T_{osc}}\right)$	$1.2\frac{K_{osc}T_S}{K_P T_{osc}}$	$3.0\frac{K_{osc}T_S}{40K_P T_{osc}}$

For a discrete PID controller, [12] states that the integral time T_I shall be

$$T_I \approx \frac{T_S}{0.1 \div 0.3} \qquad (9)$$

This requirement is easily met by the values calculated in (8).

Digital PID controller software implementation

The digital implementation of the PID controller based on equation (5) is straight forward once the P, I, D coefficients have been determined in (8).

Following C-code excerpt outlines the software implementation of the PID algorithm:

```
//define a dead-band for the error
#define epsilon 0.01
//anti wind-up for the integral sum
#define I_MAX 1000
#define I_MIN -1000
//limit the output duty cycle
#define D_MAX 95
#define D_MIN 0

#define Kp 0.499
#define Kd 0.25
#define Ki 0.015

floatPIDcal(float v_set, float v_sense)
{
  static float pre_error = 0;
  static float integral = 0;
  float error;
  float derivative;
  float dutycycle;
  //calculate the error
  error = v_set – v_sense;
  //stop integration if error smaller than epsilon
  if (abs(error) > epsilon) {integral = integral + error;}
  //anti-wind-up fort the integral sum
  if (integral > I_MAX) {integral = I_MAX};
  else if (integral < I_MIN) {integral = I_MIN};
  //calculate the derivative term
  derivative = (error - pre_error);
  //caculate PID output, duty cycle for the buck controller
  dutycycle = Kp*error+ Ki*integral+ Kd*derivative;
  //prevent output saturation
  if (dutycycle > MAX) {dutycycle = MAX;}
  else if (dutycycle < MIN) {dutycycle = MIN;}
  //update error sum
  pre_error = error;
  return dutycycle;
}
```

Experimental investigations

Based on the theoretical analysis of the discrete PID controller and the software structure considered in the previous chapters, a practical implementation and further investigation with focus on transient and stability performance promises good results.

Prototype PCB

A prototype printed circuit board has been designed and assembled according the schematic in Figure 1. Care has been taken to keep the loop area small in the discontinuous current paths in order to minimize the EMI and prevent noise coupling issues.

Fig.3. Prototype PCB, top view.

Buck converter components

For the investigation purposes of this paper the DRV8412 integrated circuit by Texas Instruments has been used for the buck switch and synchronous rectification. DRV8412 is a highly sophisticated, fully featured fast half-bridge driver, containing all the needed function blocks, including control logic, diagnostics, protection circuitry and power MOSFETs on a single chip with large exposed thermal pad [13].

The logic inputs of DRV8412 are TTL- and 3.3V-compatible and can be driven directly by a low-voltage microcontroller without the use of level shifters. Four PWM inputs accept PWM frequency of up to 500kHz, making this driver very well suited for DC/DC converter experiments with high switching frequencies. Moreover, a built-in dead-time timer prevents the high- and low side FETs from shout-through pulses. Four completely independent and fully featured half-bridge power stages are accommodated on a single chip.

The microcontroller used is a dsPIC33F derivative by Microchip. It has following important feature set:

- DSP core with 120Mhz clock; 2Msps 10-bit ADC; four high-speed, high resolution (up to 1.04ns) PWM generators with dead-time;
- Adjustable overcurrent protection for each PWM channel.

Fault condition behavior

An adjustable, fast over-current protection for the integrated FETs is also available on chip in DRV8412. This is a very important, system safety related feature.

In case of LED output short to ground or LED overcurrent condition the inductor current will rise above the set overcurrent limit. Then, the built-in overcurrent protection of DRV8412 instantly shuts down both outputs and sets its diagnostic output pin to low in order to signal a fault condition to the microcontroller. The µC can be programmed to employ a hiccup protection mode, trying to restart the buck for certain number of cycles and eventually shutting down DRV8412, if the overload condition still persists. In this application, the overcurrent threshold is set to approx. 3.5A.

Steady state operation

In steady state operation (Figure 4) the average LED current is regulated to 1000mA. A measurement indicates a negligible -0.2% error (red trace), thus confirming the properly chosen gain and integral coefficients. The execution time of the PID software, including the ADC sampling time and the threefold multiplication routines is 1.13µsec (yellow trace) – an indication that the PID control routines can be easily executed within one switching cycle of the buck converter for high regulation speed and stability. The FET switching frequency has been initially set to 217kHz (green trace).

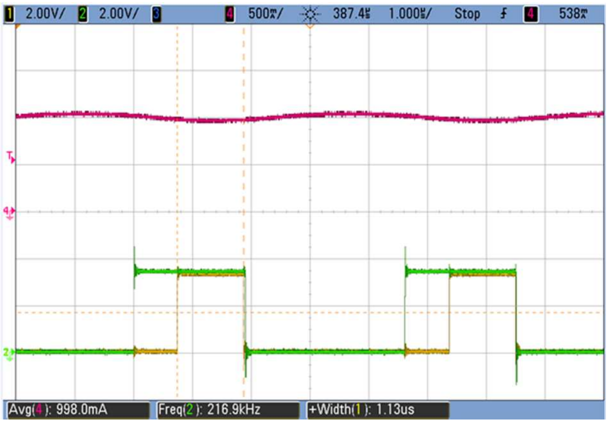

Fig.4. Steady state operation of the LED driver (red – LED current, yellow – PID controller execution time, green – PID controller output PWM).

Dynamic characteristics

The load step response of the LED controller is an important measure of its quality. The light intensity of the LEDs is usually controlled by applying a dimming PWM, typically in the frequency range 200Hz…2kHz. PWM resolution of 10 bits and more is often required.

The pulse response of the LED driver must therefore be fast enough to meet the minimum pulse width requirements which result from the PWM period divided by the number of steps for the corresponding PWM resolution.

The overshoot of the LED current during load transients is also an important issue, related to the maximum current limitations of modern high power LEDs. Due to the small thermal mass of the LED junction structures, even overshoots of short duration can increase the LED junction temperature above the acceptable limits.

The initially calculated parameter set in (8) results in a fast rise time of approx. 20µsec but also in underdamped control behavior with 19% LED current overshoot above the set-point. This might be an issue in the real-life application, since the LEDs allow for certain, relatively small current overshoot, typically in the range of 20-30%. A slight increase of K_D K_D from 0.015 to 0.022 reduces the overshoot to acceptable 4% (Figure 5).

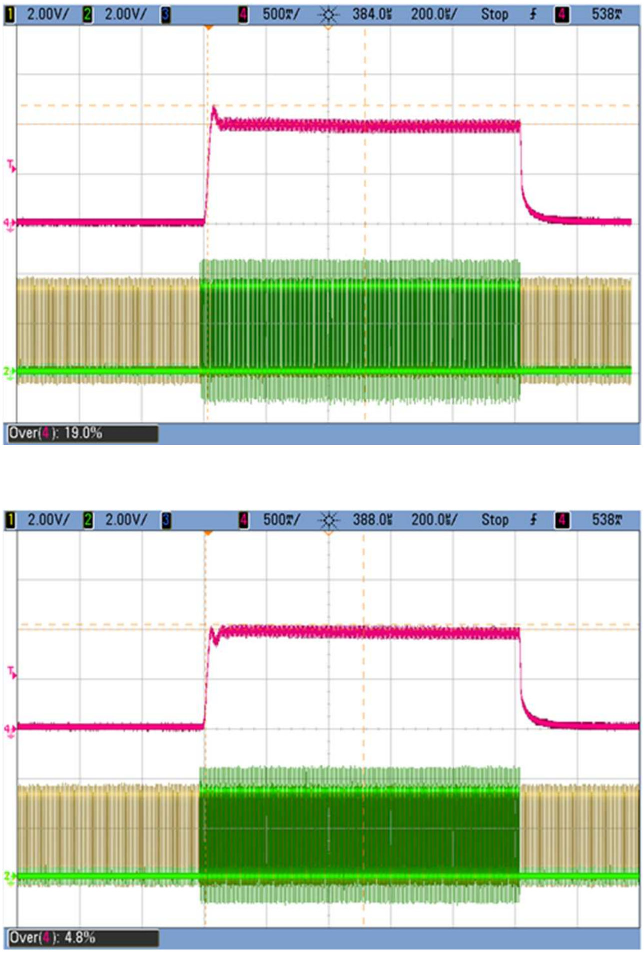

Fig.5. LED current overshoot tuning (red - LED current).

Figure 5 also indicates the physical limitations of the reaction speed of the control system, posed by the natural time constant of the buck stage LC-tank:

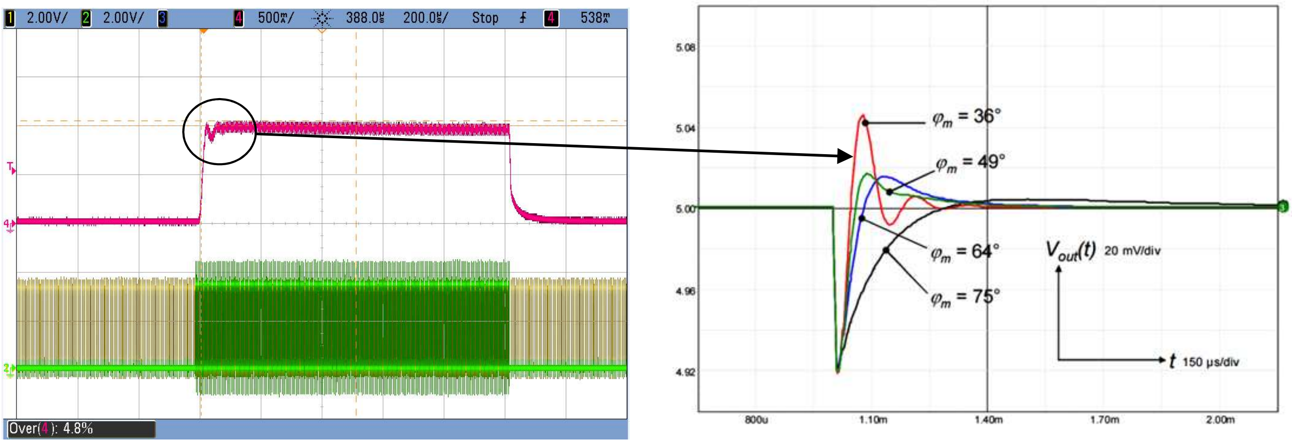

Fig. 6. Relation between transient response and phase margin according to Basso [17].

(10) $$\tau = \sqrt{LC} = \sqrt{90\mu H.4{,}7\mu F} \approx 20\mu s$$

It becomes evident that the rising and falling edges of the LED current cannot be shorter than 20µs if the energy in the inductor and the capacitor is fully depleted in the off phase. In cases where faster response times are required, e.g. in high-resolution dimming applications, an additional FET connected in parallel to the LEDs can provide very steep rising and falling times of couple of micro- or even nanoseconds [14].

Stability

The stability criteria for a closed loop control system are well established in the control theory [15], [16]. Design target is usually a phase margin close to 45°. By definition, the phase margin is the difference between the actual phase (i.e. as depicted in the Bode diagram) and -180° at the frequency, where the gain of the closed loop becomes unitary (or 0dB). This frequency determines the bandwidth of the closed control loop. The physical explanation of this requirement is that at the point where the gain of the negative feedback becomes one and noises or distortions cannot be suppressed anymore there still shall be enough phase margin to prevent a rapid phase shift to -180°. Is this condition does not hold true, the system might become instable and even start oscillating. A quick and efficient approach to investigate the stability of the closed loop controller without the use of an expensive network analyzer is to look at the load step response of the converter. For a buck converter, a relation between the

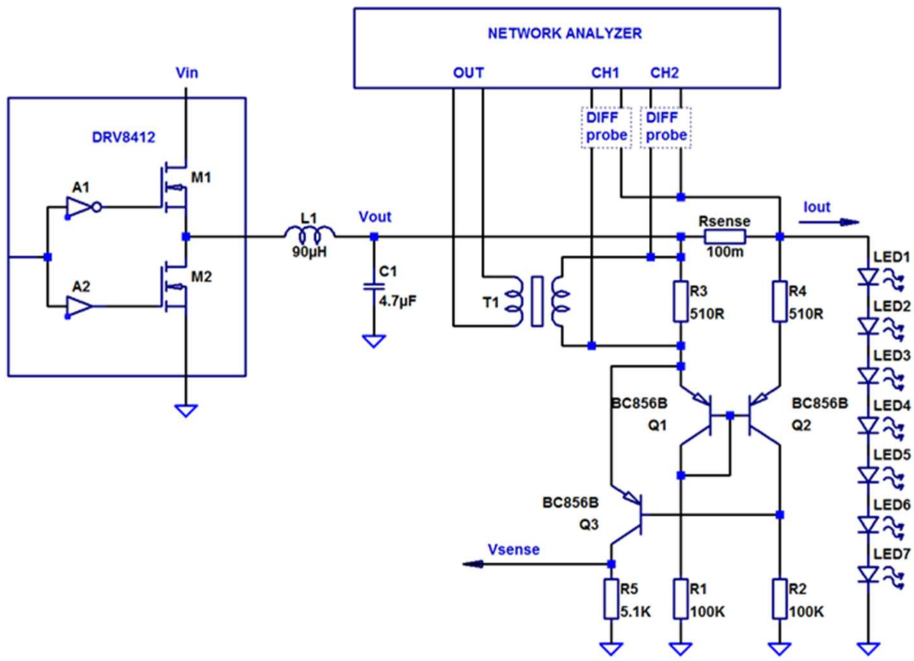

Fig.7. Closed loop stability measurement setup with vector network analyzer (VNA).

damping factor Q, the pulse shape and the phase margin can be derived [17]. A comparison of the measured LED current shape during a load step of the PID controller, tuned according to Table 1, to the diagram depicted in [17], predicts a phase margin of slightly more than 36°. This value will be compared to the phase margin measured with a vector network analyzer (Figure 6).

The classic stability investigation is based on the Bode plot of the closed loop transfer characteristic (gain and phase). A vector network analyzer (VNA) injects small-signal (mostly in the mV-range) sinus perturbations into a high impedance node of the feedback network. The excitations travel all the way along the feedback loop, two VNA measurement ports receive the incident and the reflecting wave, a DSP engine performs fast FFT and calculates the gain und phase of the closed loop response of the device-under-test (DUT).

For the experiments in this paper an Omicron Bode 100 VNA [18] has been used in following configuration (Figure 7).

The Bode plot of the tuned PID controller indicates a good phase margin of 40° at 4.5kHz crossover frequency (Figure 8).

The measured phase margin of 40° complies very well with the predicted value of slightly more than 36° according to [13]. Further improvement of the phase margin is possible on the expense of reduced controller bandwidth.

Efficiency

Efficiency measurements for different LED string lengths and currents are summarized in Table 2. The The LEDs are mounted on a large heatsink und cooled by pressurized air, the supply voltage of the buck converter is held constant at 45V level. Efficiency measurements are carried out with various number of LEDs and LED currents (Table 2).

Table 2.

Buck Converter Efficiency

Buck Converter Efficiency [%]			
# of LEDs	**LED current [mA]**		
	200	**500**	**1000**
4	89.1	92.4	91.4
5	90.9	93.3	92.9
6	91.6	94.6	93.4
7	92.2	95.7	94.1

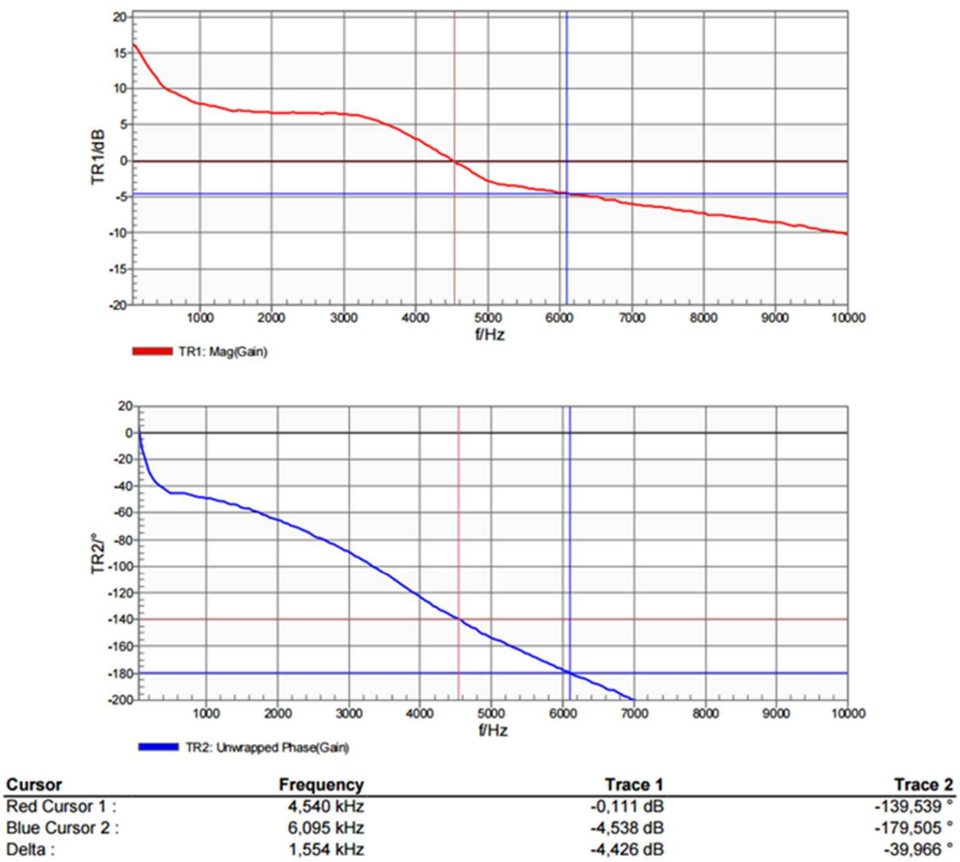

Fig.8. Bode plot of the tuned LED driver.

The graphical representation of the efficiency numbers is shown on Figure 9.

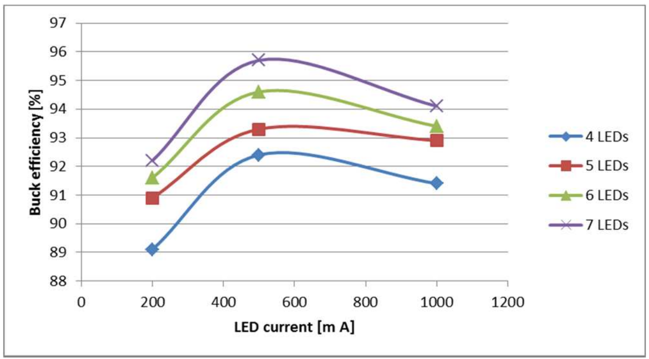

Fig.9. Efficiency plot of the tuned LED driver.

Conclusion

The digital LED driver presented in this paper performs excellently "straight of the box". It meets easily most of the design goals, stated at the beginning of this work: the steady state error is negligible, the impulse response is fast and the stability of the control system nearly meets the design target.

Further work can expand the performance of the system in following aspects:

- improvement of the phase margin by reducing the gain of the closed loop by 3…4dB. Doing so will push the phase margin to app. 55° and meet our design target, on the expense of reduced bandwidth of the controller down to approx. 4kHz;

- design of an adaptive PID controller with multiple parameter sets for start-up, shutdown and steady state. Then, the comprehensive PID algorithm only engages during start-up phase to obtain a fast transient response. In the steady-state operation, a PI controller without D-term reduces the jitter of the duty cycle and improves stability and noise suppression;

REFERENCES

[1] Infineon AG, Multitopology LITIX Power DC/DC Controller TL5098EL, Datasheet, Rev.1.2, 12.3.2015

[2] Linear Technology Corporation, 100Vin, 100Vout Multi-Topology LED Controller LT3756x, Datasheet

[3] Maxim Integrated Ltd., High-Voltage HB LED Drivers with integrated High-Side Current Sense, MAX16833x, Datasheet Rev 11, Juni 2016

[4] Texas Instruments, UCD3138128, UCD3138A64 Highly-Integrated Digital Controller For Isolated Power Rev.B , February 2017

[5] Kovatchev, E., N. Evstatieva. Analysis and investigations on a cost-efficient high-side current sensing circuit for automotive applications. Sixth International Conference on Energy Efficiency and Agricultural Engineering, Ruse, Bulgaria, 2015, pp. 452-462.

[6] PID controller. Wikipedia, [Online]. Available: https://en.wikipedia.org/wiki/PID_controller#Derivative_term. [Accessed November 2015].

[7] MathWorks, "Discrete Time Integrator," [Online]. Available: http://de.mathworks.com/help/simulink/slref/discretetimeintegrator.html. [Accessed November 2015].

[8] Ziegler–Nichols method, [Online]. Available: https://en.wikipedia.org/wiki/Ziegler%E2%80%93Nichols_method. [Accessed November 2015].

[9] Takahashi, Y., M.J. Rubins, D.A. Auslander. Control and dynamic systems, Addison-Wesley Publishing Co., 1970.

[10] Cohen-Coon PID Method, [Online]. Available: https://controls.engin.umich.edu/wiki/index.php/PIDTuningClassical#Cohen-Coon_Method. [Accessed November 2015].

[11] Isermann, R. Digital Control Systems, Berlin: Springer-Verlag, 1989.

[12] Wittenmart and Åstrom. Computer Controlled Systems – Theory and Design, New Jersey: Prentice-Hall, 1990.

[13] Texas Instruments, "DRV84x2 Dual Full-Bridge PWM Motor Driver," December 2014. [Online]. Available: www.ti.com/lit/ds/symlink/drv8412.pdf. [Accessed 2015].

[14] Dimming Techniques for Switched-Mode LED Drivers, SNVA605, Texas Instruments, Dallas, Texas, 2011.

[15] Bubnicki, Z. Modern Control Theory, Springer-Verlag Berlin Heidelberg, 2005.

[16] Ridley, R. "ridleyengineering.com," [Online]. Available: http://www.ridleyengineering.com/loop-stability-requirements.html. [Accessed 10 2015].

[17] Basso, C. The Link Between The Phase Margin And The Converter Transient Response, ON Semiconductor.

[18] Fast And Easy Measurements With Bode100, [Online]. Available: https://www.omicron-lab.com/bode-100/product-description.html. [Accessed November 2015].

***Emil Kovatchev, MSc.**, University of Ruse „Angel Kanchev", Bulgaria, 8 Studentska Str, Department of Electronics.*

e-mail: emil.kov@gmail.com

***Assoc. Prof. Nadezhda Evstatieva, PhD**, University of Ruse „Angel Kanchev", Bulgaria, 8 Studentska Str, Department of Theoretical and Measuring Electrical Engineering.*

tel.: +359 82 888 638, e-mail: nevstatieva@uni-ruse.bg

Received on: 30.04.2017